



# Adsorptive removal of Methylene Blue, from aqueous solution using Tea Waste as a Low-Cost indigenous biosorbent: Mechanism of Adsorption, Equilibrium Study, Kinetics and Isotherms

R. Sadki<sup>1</sup>, M. Dalimi<sup>1</sup>, N. Labjar<sup>1\*</sup>, G. A. Benabdallah<sup>1</sup>, S. El Hajjaji<sup>2</sup>

<sup>1</sup>Laboratory of Molecular Spectroscopy Modelling, Materials, Nanomaterials, Water and Environment, CERNE2D, ENSAM, Mohammed V University in Rabat, Morocco

<sup>2</sup>Laboratory of Molecular Spectroscopy Modelling, Materials, Nanomaterials, Water and Environment, CERNE2D, Faculty of Sciences, Mohammed V University in Rabat, Morocco

\*Corresponding author(\*), Email address: [najoua.labjar@ensam.um5.ac.ma](mailto:najoua.labjar@ensam.um5.ac.ma);

Received 13 Mar 2023,

Revised 28 Apr 2023,

Accepted 02 May 2023

**Citation:** R. Sadki, M. Dalimi, N. Labjar, G. A. Benabdallah, S. El Hajjaji, (2023) Adsorptive removal of Methylene Blue, from aqueous solution using Tea Waste as a Low-Cost indigenous biosorbent: Mechanism of Adsorption, Equilibrium Study, Kinetics and Isotherms, Mor. J.Chem.,14(3), 594-612.

**Abstract:** For the current investigation, extracted Tea-Waste has been employed without activation for Methylene Blue removing in aqueous media. The experiment has been operated under batch conditions. The impact of a variety of significant factors affecting adsorption process, of which, adsorbent particle size, adsorbent/adsorbate shaking time, adsorbent dose, pH medium as well as the adsorbate initial concentration on Methylene Blue removing were investigated for optimization of the process according to the One Factor At a Time approach. The laboratory results revealing that this process is both spontaneously occurring and feasible. It has been demonstrated that maximal removing percentage ( $R$ ) of 78.92 % was obtained at a maximal experimental adsorption capacity ( $Q_{m,exp}$ ) of 7.892 mg.g<sup>-1</sup>. Methylene Blue adsorptive to Tea-Waste was according to the ( $S$ -class) isotherm. The Pseudo-Second-Order Kinetic Model agrees perfectly with results, with an adsorption capacity calculated ( $Q_{e,cal}$ ) of 7.194 mg.g<sup>-1</sup>. Also, we can affirm a best fitting adsorptive process through Langmuir's isothermal model, this confirms an adsorptive effect occurring in homogeneous area of Tea-Waste. Maximum calculated adsorption capacity ( $Q_{m,cal}$ ) defined by using Langmuir's has proven up to 14.085mg.g<sup>-1</sup>. Consequently, the research suggests that Tea-Waste is a highly interesting option for efficiently treating real wastewater polluted by Methylene Blue.

**Keywords:** Methylene Blue; Tea-Waste; Biosorbent; Batch adsorption; kinetics; Isotherms

## 1. Introduction

During the last years, synthetic dyes have been applied in numerous sectors of industry to hue their products, like the textile, papermaking and dyeing of leather, as well as in the foods and cosmetics in the beauty industry, which consumes significant water resources (Varjani *et al.*, 2006). As a result, they are producing wastewater with high dyes levels that are directly entering the environmental ecosystem, becoming a serious ecological concern (Hamad and Idrus, 2022). In context of its output or production and employment, the accelerated expansion of the manufacturing of textiles has given rise to an ominous circumstance where additional environmental damage is

being done by contaminants contained in the wastewater effluents processed by the company, especially by colorants (Pathania *et al.*, 2017). The existences of extremely minor dye levels within surface waters are highly perceptible and not acceptable. Eliminating contaminant from dye reagents and excessive exposure in water surfaces poses significant risks to the aquatic ecosystem and to people living near the contaminated source of water (Boumya *et al.*, 2021; Salahat *et al.*, 2023). The synthetic dyes are recognized as environmentally hazardous and persistently, therefore require physical and chemically based processes to eliminate it from the environment (Arumai, 2008; Alam *et al.*, 2018; Yaseen and Scholz, 2019; Loulidi *et al.*, 2020).

In recent decades, the disposal of synthetic dyes from polluted water systems is becoming an increasingly significant effort to protect a sustainable environment for waters resources. Most synthetic colorants have low biodegradability and resist against environmental effects, creating major wastewater treatment problems. A number of alternative processing approaches have been employed to treat dye-containing wastewaters, but these methods are varied by efficacy, financial-cost, and by their effect on the environment (Crini, 2006). Generally, synthetic dyes removal from water resources is often carried out with a process of oxydation, precipitation, ion exchanges, electro-chemistry, ozonation, Fenton's reagents, sodium hypochloride, coagulation-flocculation, ultrafiltration/nanofiltration, biological processes and adsorption technology (Crini, 2006; Robinson *et al.*, 2001; Gupta and Suhas, 2009; Singh and Arora, 2011; Koyuncu and Güney, 2013; Holkar *et al.*, 2016; Ahmed *et al.*, 2017; Crini and Lichtfouse, 2019; Collivignarelli *et al.*, 2019).

The latter approach is considered the most cost-effective and simplest method widely used (Elmontassir *et al.*, 2019; Ait Hmeid *et al.*, 2021), in which the application of commercial activated carbons is one of the commonest adsorbents employed in the water treatment plant and was shown as a very successful process to remove dyes from effluents of waste water (Mulushewa *et al.*, 2021). Although activated carbons are a favoured adsorbent to remove dyes, their larger scale applicability is limited due to their relatively higher costs (Vital *et al.*, 2016; Shu *et al.*, 2017; Piaskowski *et al.*, 2018; Hassan and Carr, 2021; Akartasse *et al.*, 2022). This pushed the scientists to find other ways to find economical, unconventional sources of adsorbents, including agriculture residues or co-products, and also animals and wood-based materials, that are successful adsorbents of a large variety of contaminants due to their high number of active groups (Hassanein and Koumanova, 2010; Mejbar *et al.*, 2019; Kali *et al.*, 2022). Additional benefits which qualify them as good prospects are their ability and their rating in adsorbing ionic contaminants like dyes, the highest level of selectiveness to various contaminants, as well as fast kinetic (Muhammad and Abdurrahman, 2020). Other adsorbents, non-conventional low-cost materials are great biowastes sources of dye treatment as they are renewable sources and due to their natural abundance, low toxicity and because they are widely applied with or without a little processing (Franca *et al.*, 2009).

In Morocco, the Tea-Waste residues it is a domestic waste disposed of in large quantities and are disposed of like solid-waste, causing a number of problems for the environment. This is a pollutant that requires oxygen. In addition, his biodegradability requires a long period of time. Hence, a suitable methodology is needed to handle the disposition challenge. On the other side, the application of this cheaper resource as adsorbents will help to solve the problems (Uddin *et al.*, 2009). If the Tea-Waste material utilized for adsorption reaches saturation, it is simply conducted to incineration. The waste tea cinders resulting from incineration are not a pollutant but can serve as adsorbents. Tea-Waste are therefore a very economically adsorption material.

Methylene Blue is widely used for its intense color as an azo colorant in the industry of textiles for colouring of wool and natural fiber (Trifi *et al.*, 2021; Sun *et al.*, 2021; Raiyaan *et al.*, 2021). He

is further utilized in the fabrication of paintings and printers' inks. Methylene Blue is a carcinogen and was categorized to be a persistent chemical due to the fact that it is badly degraded by microorganisms, is not biodegradable and could stay in several environmental media. It is extremely poisonous to humans and animals (Hummadi *et al.*, 2022; Alam *et al.*, 2022).

In the aims to remedy the pollution of the water with reagents synthetic dyes applied in textiles industries, the purpose of this working document is to study and explores applicability for extracted Tea-Waste as natural adsorption materials for Methylene Blue removal in aqueous media and to maximize removing processing factors by statistics. During this study, we varied several experimental kinetic variables including particle size, initial concentration, shaking time, pH and adsorbent dose, to examine their influence.

The data from the laboratory research have been evaluated to assess the existence of the equilibrium, kinetic/isotherm models of adsorptive processing of extracted tea waste with no activating (Wang and Guo, 2020; El-Bindary *et al.*, 2020; Nandiyanto, 2020). The adsorption equilibrium was represented with isotherm adopted by Giles *et al.* (1974) classification. The adsorption kinetics has been analyzed with various adsorption kinetic models which include Zero-Order, Pseudo-First-Order as well as Pseudo-Second-Order. Furthermore, in this study adsorptive capacity was determined as well as elucidated using adsorption isotherm theories (Wang and Guo Han *et al.*, 2006; Quansah *et al.*, 2020; Elsherif *et al.*, 2020) like the Langmuir (1916) or Freundlich (1906) models. Adsorption isotherms are commonly employed as a means of judging the character of the adsorptive mechanism, as these may indicate the adsorbent's superficial characteristics, as well as the distribution of pores as interaction occurs within adsorbent and adsorbate. Langmuir and Freundlich equations have been identified as having a correlation coefficient values with good accordance.

## 2. Materials and methods

In the present investigation, Tea-Waste (TW) like a local and inexpensive material was employed in absorption to removing the Methylene Blue (MB) dyes in aqueous medium. Every reagent used during our work is of analytic quality. The distilled-water has been employed throughout this work. In each experiment, triplicates have been performed and averages values have been considered for data points.

### 2.1 Chemicals, reagents, solutions and matter-materials used

The Hydroxide of sodium (NaOH) and hydrochloric acid (HCl) have been utilized with no additional purifying for solutions pH adjustment. Ethanol (C<sub>2</sub>H<sub>5</sub>OH) with 96% purity was used as an extraction solvent.

### 2.2 Adsorbate

The basic dye (MB) has been applied as adsorbate for determining the adsorptive efficiencies of (TW) as adsorbent. Their properties and characteristics are given below (Table 1). (MB) was obtained from (Merck India Ltd, purity of  $\geq 95\%$ ) that has been utilized with no additional purifying. The stock solutions of (MB) dye with 1mg.L<sup>-1</sup> as initial concentration has been obtained by dissolving 1g from (MB) into 1L of distilled-water. Measuring pH in stock solution gives a pH at 5.9. However, the experimental solutions with concentrations ranging between 5 and 20mg.L<sup>-1</sup> have been obtained through dilution of the (MB) stock of solutions to accurate proportions, the distilled-water was used for necessary dilutions.

**Table 1.** Methylene Blue (MB) properties.

<b>Characteristics</b>	
Common commercial name	Methylene Blue
Type of dye class	Cationic thiazine dye
Symbol	MB
Colour Index name	Blue 9, Basic (BB 9)
Colour Index number	52,015
Melting point	100 to 110°C
Molecular Formula	C <sub>16</sub> H <sub>18</sub> ClN <sub>3</sub> S
Molecular mass	319.86g.mol <sup>-1</sup>
Molecular volume	241.9cm <sup>3</sup> .mol <sup>-1</sup>
UV-Visible spectra (maximum adsorbance wavelength)	664nm

### 2.3 Adsorbent preparing

As adsorbent, a quantity of bulk (TW), are collected without sugar without mint, and then minced up in smaller fractions, wash, drying, grinding and sieving them prior to being used for the adsorptive processing. (TW) was firstly rinsed in distilled-water repeatedly to displace any attached impurities, contaminants and impurities from its surface. After a natural drying in the sun-light (ambient conditions) for 3 days, the (TW) was drying at 105°C in an oven for 24h thus that all moisture has been removed, and was stored in a desiccator to be used for the later adsorption experiments.

Solid sample (60g) of material was milled, than the ground material is subjected to extraction. After having dried at 40°C the (TW) that has gone through an extraction, the material is separated and sieved for obtaining (TW) material having particles size equivalent to 125 and 250µm. This adsorbent material has been separated in tree samples on the basis of various particle size ranges using sieves. These materials are grouped into finest-finer (≤125µm), fine (≤250µm) and coarser lightly milled (≥250µm) which are presented in **Table 2**. These obtained samples have been dry to 60°C a minimum during 24-48 hours, then stocked to be used later in the adsorption treatment.

**Table 2.**(TW) samples grain size ranging.

<b>Material</b>	<b>Sieving (µm)</b>	<b>Particle size Distribution (µm)</b>
Finer	Passing through sieve no. 125	≤125
Fine	Passing through sieve no. 250	≤250
Coarse (lightly milled)	Retained on sieve no. 250	≥250

### 2.4 Experimental protocol: Optimisation of adsorption characteristics of MB removal

The adsorptive mechanism consists of adsorbent (TW) and adsorbate (MB) surfaces interactions. The factors affecting adsorption process are the adsorbent particle size, the adsorbent/adsorbate shaking time, the adsorbent dose, the pH medium and the adsorbate dye initial concentration. For optimizing the (MB) adsorbate removal processes and improving efficiency, a batch adsorption experiments are conducted. The approximate optimal values for these different parameters have been estimated using the “*One Factor At a Time methodology*” (**Table 3**).

Dye removing depends in direct relation with adsorbent surface-area that depends on their particle sizes. Adsorption tests have been performed with three various size portions of (TW) material (≤125µm, ≤250µm and ≥250µm). Studies of exposure time influence on the level of fixation of (MB) and removing onto (TW) was used for determining the time for equilibrating which corresponds to adsorbate/adsorbent saturating point. The adsorption of (MB) is followed with period varied at four levels from 10 to 40 minutes. In addition, the variation of (MB) adsorbate fixation level versus (TW) adsorbent mass is shown. For determining adsorbent optimum mass required for

removing (MB), a tests series was performed at different masses of (TW) varying between 0.01 and 0.05g. The pH medium effect in adsorptive process can be considered as the most critical parameters and an important factor primarily used in any adsorption study for determining the optimum conditions to remove the dyes. The pH of the solution influences the adsorptive capacity since this has significant impacts regarding the adsorbent surface characteristics and also the dye types contained on the solution, as well as, the adsorption mechanism. For the purpose of evaluating the influence of pH on the adsorptive performance and identifying optimal pH, adsorptive of (MB) on (TW) was performed with pH values between 2 and 11. (MB) adsorbate initial concentrations are an important factor in the adsorptive performance. For the purpose of determining (MB) concentration at equilibrium, we made variations of the concentrations between 5 to 20mg.L<sup>-1</sup>.

**Table 3.** Detailed procedures for batch adsorption experiment parameters.

Investigated effects	Control factors	Variable factors
Adsorbent particle size	(MB) initial concentration: 10mg.L <sup>-1</sup> Adsorbent dose: 0.01g Shaking speed: 250rpm Contact time: 30min Volume: 25mL Solution pH: 5.9	Adsorbent particle size (µm): 125, 250 and Lightly milled
Adsorbent/adsorbate contact time	(MB) initial concentration: 10mg.L <sup>-1</sup> Adsorbent dose: 0.01g Adsorbent particle size: 250µm Shaking speed: 250rpm Volume: 25mL Solution pH: 5.9	Contact time (min): 10, 20, 30 to 40
Adsorbent dose	(MB) initial concentration: 10mg.L <sup>-1</sup> Adsorbent particle size: 250µm Contact time: 40min Shaking speed: 250rpm Volume: 25mL Solution pH: 5.9	Adsorbent dose (g): 0.01, 0.02, 0.04 and 0.05
pH medium	(MB) initial concentration: 10mg.L <sup>-1</sup> Adsorbent dose: 0.05g Adsorbent particle size: 250µm Contact time: 30min Shaking speed: 250rpm Volume: 25mL	Solution pH: 2, 3, 4, 5, 6, 7, 8, 9, 10, 11
(MB) adsorbate initial concentration	Adsorbent dose: 0.05g Adsorbent particle size: 250µm Contact time: 30min Shaking speed: 250rpm Volume: 25mL Solution pH: 5.9	Solution concentration (mg.L <sup>-1</sup> ): 5, 10, 15, 20

We conducted all (MB) batch adsorptive investigations in room temperature. These investigations have been conducted within a set of 50mL from flask containing (TW) adsorbent and the solutions of (MB) of 25mL. These flasks were shaking till the equilibrium of the suspensions is reached, then the samples are centrifuged to remove the supernatant. After decantation and filtration, MB concentrations for each variable parameter are measured using (UV) Spectrophotometry. Removal efficiency (*R*) or removal percentage (%) of (MB) in addition to adsorption capacities at equilibrium (*Q<sub>e</sub>*) was estimated.

## 2.5 Methylene Blue adsorption equilibrium: Theory and calculation

The adsorption mechanisms at equilibrium are expressed by their isothermal behavior, the type of which allows explaining qualitatively adsorbate/adsorbent interactions. This study describes mathematics of the isothermal equations based on: (i) the Giles et al. classification, (ii) the adsorption kinetics and (iii) isotherm models, to better understand the adsorptive materials' performance toward the adsorbates.

### 2.5.1 The Giles classification of adsorption equilibrium diagram applied for description of experimental data

In the adsorptive process, a dynamical equilibrium occurs between the molecules of adsorbate in aqueous solutions and the adsorbed molecules by surface sites of the adsorbent. Continuously the adsorbate molecules are adsorbing and desorbing from the adsorbent surface. By the time the adsorptive and desorptive rates balanced, a dynamic stability is reached. This state of equilibrium is usually described as an isotherm, a graph that shows the adsorptive equilibrium. It is the curve binding, by relating adsorptive capacities at equilibrium ( $Q_e$ ) to (MB) concentrations at equilibrium ( $C_e$ ). Several authors have proposed a classification of adsorption isotherms based on their curvatures and their initial slope. This is an essential stage in identifying an appropriate model which may be utilized for designing decisions. In this study, we are going to demonstrate that the aspect of adsorption equilibrium data could be connected to the mathematic forms of the isothermal equations with the classification of Giles et al., Based on their forms Giles *et al.* (1974) classify adsorptive isotherms in four categories. Giles et al., have differentiated isotherm classes into (**H**) high affinity, (**L**) Langmuir, (**C**) constant partition and (**S**) sigmoidal. In general, isotherms of (**S-class**) show a concave form in the lowest concentrations, the slope must be maintained as the concentration approaching 0. There are two explanations for the isotherms of (**S-class**). One, "solute-solute" force of attracting to the surface can induce adsorptive collaboration leading to the (S)-form. Two, solute adsorptive can be blocked due to the concurrent reactions in their solutions, like a ligand-complexing reactions. Whereas the (**H-class**) and (**L-class**) isotherms show a convex form, the (**H-class**) isotherm attains higher slopes while the slopes of the (**L-class**) isotherms are maintained constantly. That is indicative of the increasing adsorptive affinity of the (**H-class**) isotherms as the concentration is decreased. The (**C-class**) isotherms have a constant adsorptive affinity over the wide range of concentrations, represented by the straight curve in the graphs ( $Q_e$ ) vs ( $C_e$ ). The classification consists of a purely observational approach not revealing the procedures leading to the various forms of isotherms. Adsorptive analyses were carried out at variable (MB) adsorbate initial concentration being 5, 10, 15 & 20 (mg.L<sup>-1</sup>) according to the experimental design given on the [Table 4](#).

**Table 4.** Experimental parameters for the equilibrium adsorptive Giles et al., classification.

Control factors	Variable factors
Adsorbent dose: 0.05g	Solution concentration (mg.L <sup>-1</sup> ):
Adsorbent particle size: 250µm	5, 10, 15 and 20
Contact time: 30min	
Shaking speed: 250rpm	
Volume: 25mL	
Solution pH: 5.9	

### 2.5.2 Adsorption kinetics at equilibrium

Adsorptive kinetics has been employed for exploring the adsorptive rate and mechanisms, possibly occurring because of both physically and chemically induced phenomena, and for

comparison through laboratory results. The adsorption kinetics investigation has been performed for understanding the adsorptive and contact time relations at equilibrium, which determines time necessary to reach the equilibrium of the adsorptive operation. Adsorptive laboratory results have been accurately matched in some of the adsorptive kinetics model applied in different researches. Several kinetic models may provide some indication of the adsorptive routes and the likely processes implied. Furthermore, it is an interesting input for the process developing of the adsorptive process as well as for their design. For understanding the adsorptive behavior of (MB) on the adsorbent (TW), in present study, we have taken zero-order, pseudo-first-order in addition to pseudo-second-order kinetics model. These kinetics models of adsorption represent the more commonly kinetic models employed monitoring kinetics in adsorptive processes. A relative higher value of ( $R^2$ ) coefficients of correlation indicates a successful model for describing (MB) adsorptive kinetics. Respectively, the coefficients of the adsorptive kinetics models are predicted by plotting ( $C_t$ ) as a function of ( $t$ ),  $\ln(Q_e - Q_t)$  according to ( $t$ ) in addition to ( $1/Q_t$ ) according to ( $t$ ), with respect to the kinetics models (Zero-Order, Pseudo-First-Order & Pseudo-Second-Order).

Adsorptive kinetics investigations have been performed at variable adsorbent/adsorbate contact time ranging of 10, 20, 30 to 40 minutes, according to the experiment plan presented on [Table 5](#).

**Table 5.** Experimental conditions to analyse the adsorptive kinetics.

Control factors	Variable factors
MB initial concentration: 10mg.L <sup>-1</sup>	Contact time (min):
Adsorbent dose: 0.05g	10, 20, 30 to 40
Adsorbent particle size: 250 $\mu$ m	
Shaking speed: 250rpm	
Volume: 25mL	
Solution pH: 5.9	

### 2.5.3 Equilibrium adsorptive isotherms

Analyzing the adsorptive isotherm will give an existing equilibrium relation of adsorbate and adsorbent. The adsorptive processing analyzing and designing necessitates a proper adsorptive equilibrium for the best understanding of this adsorptive processing. The adsorptive equilibrium gives basic physical and chemical data to evaluate the applications of the adsorptive operation as a unitary process. For designing the treatment procedure for the wastewater from industry, experimental adsorptive data will have to be adjusted with isotherm models to obtain a suitable one. For the current investigation, commonly employed isothermal models, specifically that of [Langmuir \(1916\)](#) in addition to [Freundlich \(1906\)](#) one, have been applied for analyzing the experimentally obtained equilibrium results and estimating the maximal adsorptive quantity at equilibrium ( $Q_m$ ).

(i) Langmuir isotherm model: It has been elaborated on 1916 ([Langmuir, 1916](#)), it is considered as the adsorptive isotherm mostly employed, describes monolayer adsorptive and assumes that adsorption occurs on uniform adsorbent areas with no trans-migration occurring from molecules adsorbed within neighboring areas. It is represented by linear shape from Langmuir isotherm, in which values for Langmuir constant ( $K_L$ ) and ( $Q_m$ ) may be approximated using a non-linear computation by plotting ( $1/Q_e$ ) versus ( $1/C_e$ ) in which ( $Q_m$ ) is the inverse of the slope and ( $K_L$ ) is estimated by the intercept. The adsorptive preferrability of (MB) over (TW) has been studied via one dimension constant known as the separation coefficient ( $R_L$ ) (or parameter of equilibrium) which can be determined from the Langmuir isotherm model. The Langmuir isothermal model is advantageous if the value of ( $R_L$ ) ranges from 0 to 1, it is disadvantageous, linearly or irreversibly when  $R_L > 1$ ,  $R_L = 1$ , and  $R_L = 0$ , respectively.

(ii) Freundlich isotherm model: Furthermore, it has been elaborated in 1906 (Freundlich, 1906) and its empirical equation frequently applied to describe the multilayer adsorptive process on heterogeneous surface energy systems (non-ideal adsorption), in which adsorbed particles are interacting intensely together, with no ( $Q_m$ ) required. Both Freundlich constant ( $K_F$ ) and adsorbent adsorptive intensity ( $n$ ) may be computed through non-linear regression. Similar to the Langmuir isotherm, these constants can be estimated by tracing  $\ln(Q_e)$  versus  $\ln(C_e)$ , and ( $K_F$ ) by intercept and ( $n$ ) by slope. ( $n$ ) values being in the range of 1 to 10 showing an advantageous adsorptivity. An indicator of the favours of the adsorbent/adsorbate systems is given by the magnitude of ( $1/n$ ). In general, ( $1/n$ ) values range from 0 to 1, which illustrates nonlinearity in relation between dye solution concentration and adsorptive. When  $1/n=1$ , adsorption becomes linearly, and another way to look at it is to imply chemical ( $1/n<1$ ) or physical ( $1/n>1$ ) adsorptivity. Also,  $1/n<1$  suggested (MB) favorableness adsorptivity on the adsorptive area of (TW).

Adsorptive isotherm investigations have been performed at varying (MB) initial concentration ranging between 5 and 20mg.L<sup>-1</sup>, as per the experimental design presented in the Table 6.

**Table 6.** Analysis of adsorptive isotherms experimental conditions.

Control factors	Variable factors
Adsorbent dose: 0.05g	Solution concentration (mg.L <sup>-1</sup> ):
Adsorbent particle size: 250 $\mu$ m	5, 10, 15, 20
Contact time: 30min	
Shaking speed: 250rpm	
Volume: 25mL	
Solution pH: 5.9	

## 2.6 Devices used and characterization techniques

The quantity used of the dried (TW) is 60g which first goes through an electric grinding using a laboratory blender (Conair Waring), the particles obtained are of medium size. This milled material undergoes an extraction by the Soxhlet method. The solid sample is mixed with 250mL of an appropriate solvent, using a hydroalcoholic solution composed of: distilled water/ethanol (25/75%) and placed in a Soxhlet extractor. The temperature is adjusted to 60°C for 5 hours. The extract is then dried and concentrated. After extraction the material was dried at 40°C, then sieved in a laboratory electromagnetic sieve shaker (BA200N, CISA), for 4 min, with a vibration amplitude of 1.5mm, to obtain two (TW) separates granulometric particles with 125 and 250 $\mu$ m sizes and stored for use in the later adsorption experiments. All solutions had been adjusted for pH with (HCl) and (NaOH) by employing a pH Meter (by PHS-3BW Benchtop), equipped with a calibrated pH glass electrode. Batch adsorption investigations have been performed in flasks and agitated at 250rpm shaking speed and room temperature until the equilibrium is reached. A magnetic rotational orbital agitator has been employed for facilitating intimating contact of the adsorbent (TW) to dye (MB). After equilibrating the suspensions, the optical densities (absorbance) in different aqueous solutions of (MB) of all parameters have been estimated by means of UV-1900, UV-vis spectrophotometer (Shimadzu) to  $\lambda_{max}$  of the 664nm for determining the equilibrium concentration of (MB). This concentration has been estimated and interprets based on the initial pre-calibrated calibration graph of absorbance as a function of (MB) concentration ranging between 2 and 10mg.L<sup>-1</sup>. Finally, removing percentage of (MB) has been calculated.



### 3. Results and discussion

#### 3.1 TW adsorbent particle size effect

The experiment (Figure 1) showed that as the particle size of TW reduces between slightly milled >250 to 125  $\mu\text{m}$ , removing efficiencies increased through 13.09 to 39.45%, also adsorption capacity ( $Q_e$ ) is increased between 3.273 and 9.863  $\text{mg}\cdot\text{g}^{-1}$ . Furthermore, removability efficiencies increasing as particle size decreases resulting from the increase in (TW) adsorbent active sites on surfaces according to this order, this was predictable as adsorptive is a surface phenomenon, therefore small size particles provide relatively higher surfaces sites and accordingly high adsorptive under equilibrium. Here we could see a large (TW) size of the particles impact on (MB) adsorption, the removing efficiency is important for the finest particle size 125  $\mu\text{m}$  and decrease with increasing particle size 250  $\mu\text{m}$  and without sieving (slightly milled). From this experiment, for (MB) removal on a (TW) adsorbent it was possible to determine as favorable parameter, the optimum particle size of the order of 125  $\mu\text{m}$ , with a removal percentage ( $R$ ) of 39.45% and an adsorption capacity ( $Q_e$ ) to 9.863  $\text{mg}\cdot\text{g}^{-1}$ .

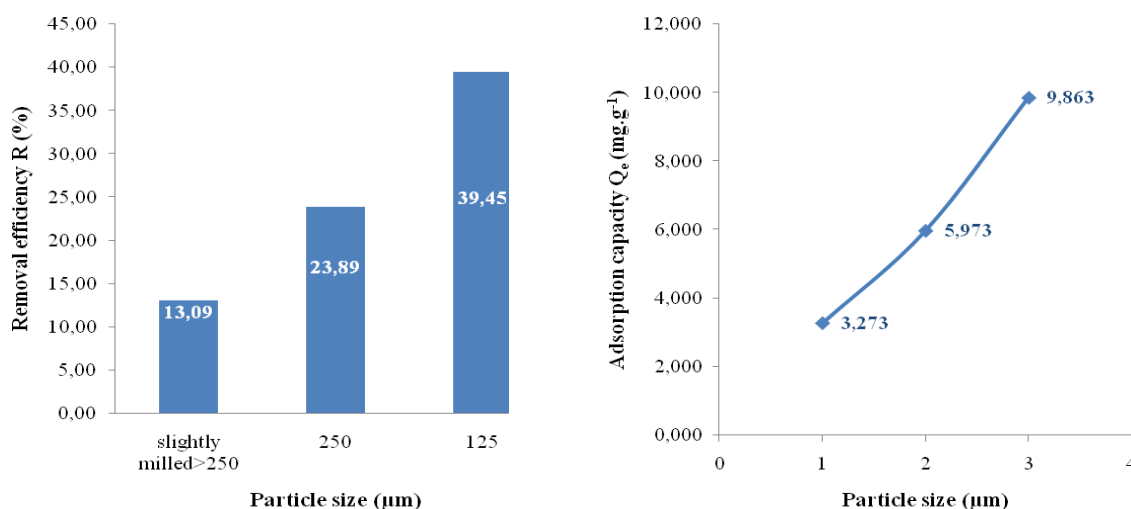
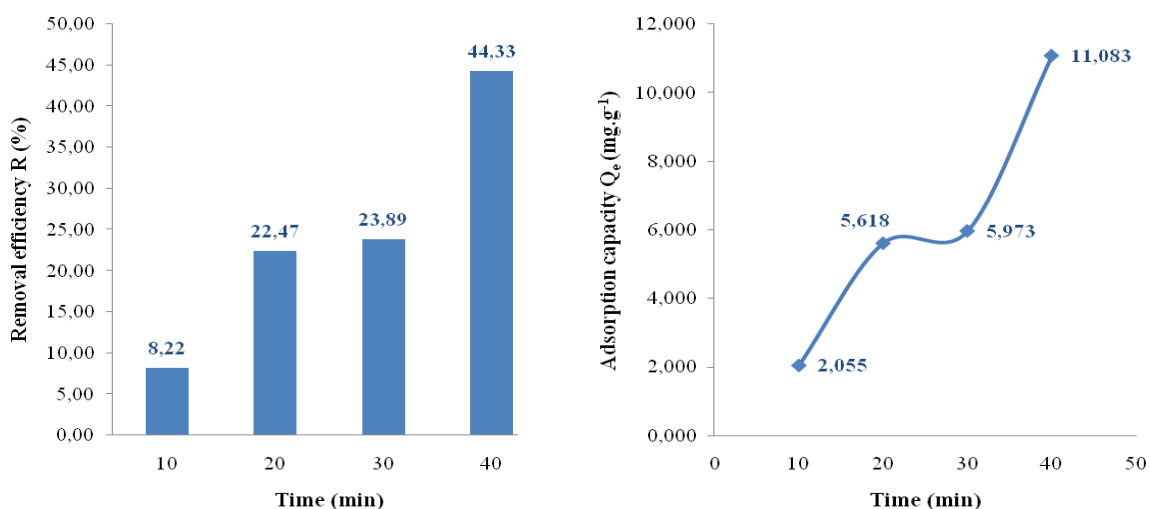


Figure 1. (MB) adsorption on (TW) at variable particle size.

#### 3.2 Contact time effect

Findings reported in Figure 2 show that there is a quick increasing efficiency of (MB) removal within the initial 20 minutes of contact, reaching a removal percentage ( $R$ ) of 22.47% with an adsorption capacity ( $Q_e$ ) at 5.618  $\text{mg}\cdot\text{g}^{-1}$ . However after this point, the adsorptive processing has been slowing and remains approximately constant between the contact times of 20-30 min, indicating a state of equilibrium, to reach only a removal percentage ( $R$ ) of 23.89% and an adsorption capacity ( $Q_e$ ) to 5.973  $\text{mg}\cdot\text{g}^{-1}$  at contact time of 30min with only 1.42% removal of (MB) was obtained. Then, (MB) elimination increases rapidly after 40min of contact, reaching a removal percentage ( $R$ ) of 44.33% and an adsorption capacity ( $Q_e$ ) at 11.083  $\text{mg}\cdot\text{g}^{-1}$ . From showing results, we can deduce that the contact time has a significant contribution in removing (MB). The efficiencies of removing are increased with increasing contact time as a result of increasing time availability for adsorptive complex formation occurring within the (MB) and the adsorbent (TW). In fact, on economic terms, the rapid adsorptive kinetics ensures a higher percentage of removal for industrial companies. Therefore, for (MB) removal on a (TW) support it was possible to determine as favorable parameter, the contact time of the order of 40min, with a removal percentage ( $R$ ) of 44.33% and an adsorption capacity ( $Q_e$ ) to 11.083  $\text{mg}\cdot\text{g}^{-1}$ .



**Figure 2.** (MB) adsorption on (TW) at variable contact time.

### 3.3 Effect of adsorbent dose

Experimental findings shown in **Figure 3**, indicated that the amount of (MB) adsorbed increases as the (TW) adsorbent mass increases, between 0.01 and 0.02g from 44.33 to 56.20% as removal percentage ( $R$ ). Fast increasing could be deduced as the mass (TW) is augmented in the range of 0.02 to 0.05g, from 56.20 to 75.82% as removal percentage ( $R$ ). In fact, an important increasing of the adsorbed quantity of (MB) noticed depending on the mass of the adsorbent (TW) is caused by the increasing of total adsorbent surfaces sites and thus available number of activated surfaces for the adsorptive process, that grows according to the high dosage of the adsorbent (TW) reaching the mass 0.05g. Nevertheless, there was an inverted tendency of the adsorption capacity ( $Q_e$ ) was found. The curve in the figure indicates clearly an inverse and drastic decrease of the adsorption capacity ( $Q_e$ ) of 11.083 to 3.791 mg.g<sup>-1</sup> when the adsorbent dose is increasing by 0.01 and 0.05g. In addition, continuous diminution of adsorption capacity ( $Q_e$ ) as the dose of adsorbent (TW) increases could result from 2 causes. First, a cohesive interaction between the adsorbent particles likes aggregation or agglomeration as a result of a higher dose of adsorbent being added thus resulting in a significant reduction in the effective surface sites by weight (g) of the adsorbent in addition an increasing of the distribution path length, leading to limiting the adsorption process. Secondly, the unsaturation of (TW) adsorbent active sites occurs with greater dosing, as a result of the excessive availability of adsorbent compared to what is needed, although the adsorptive capacity depends in inverse order to the dosing of the adsorbent. Our obtained findings can be considered in line with the ones observed in several works concerning the adsorptive properties of (MB) or other cationic dyes on other types of adsorbents. Considering all favorable and unfavorable effects that increase in (TW) dose has on removal efficiency ( $R$ ) in addition to adsorption capacity ( $Q_e$ ), a reasonable and ideal adsorbent amount of 0.04 g for 25mL of solution volume has been required for (MB) removal. That dosing of adsorbent corresponding to a removal percentage ( $R$ ) of 66.35% and to an adsorption capacity ( $Q_e$ ) of 4.147 mg.g<sup>-1</sup>, with an initial (MB) concentration of 10 mg.L<sup>-1</sup>.

### 3.4 Solution pH effect

**Figure 4** presents pH of aqueous solution, showing how the pH is related to the removal of (MB). These results demonstrates a progressive increasing of the amount of (MB) adsorbed with increasing solution pH, between value of pH from 2 to 5, from 37.56 to 81.94% for removal

percentage ( $R$ ), and from 1.878 to 4.097 mg.g<sup>-1</sup> for adsorption capacity ( $Q_e$ ). After this, the adsorption process slowed and remains approximately constant between the pH values from 5 to 6, indicating a state of equilibrium, to reach a removal percentage ( $R$ ) of 81.83% and having an adsorption capacity ( $Q_e$ ) at 4.069 mg.g<sup>-1</sup> at a pH around 6. However, the adsorption decreases as the pH increases further.

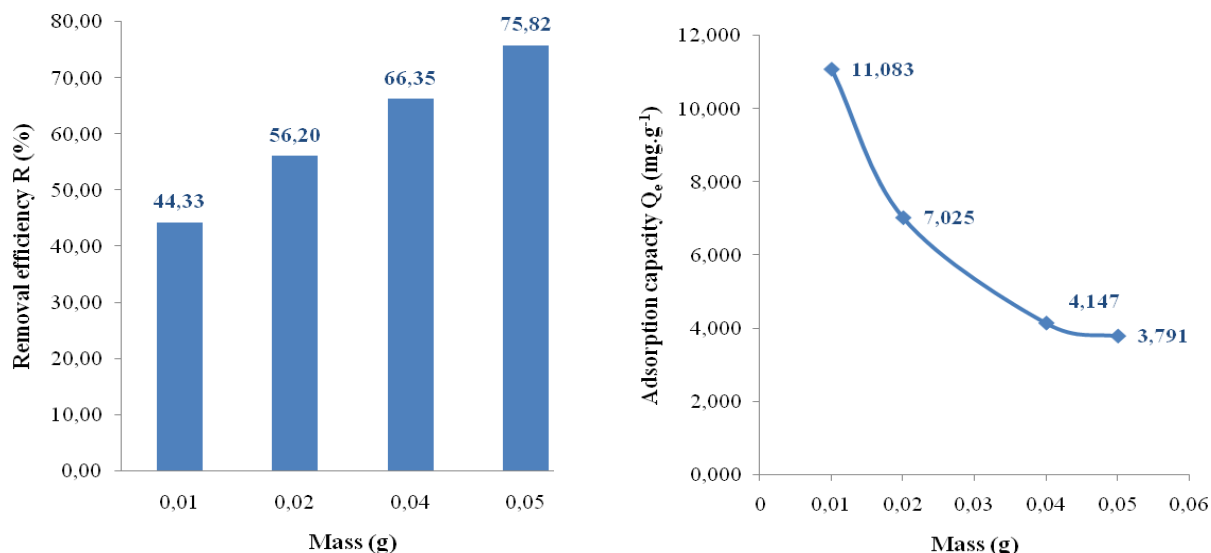


**Figure 3.** (MB) adsorption on (TW) at variable variable Mass's.

Until the pH values from 7 to 8 where the adsorption decreases rapidly, to reach at the pH value of 9 a removal percentage ( $R$ ) of 47.28% and an adsorption capacity ( $Q_e$ ) equal to 2.364 mg.g<sup>-1</sup>. Suddenly, adsorptive capacity increases at the pH values of 10, to reach 84.34% for removal percentage ( $R$ ), and 4.217 mg.g<sup>-1</sup> for adsorption capacity ( $Q_e$ ), and then it goes to the highest at the pH values of 11, to reach 85.10% for removal percentage ( $R$ ), and 4.255 mg.g<sup>-1</sup> for adsorption capacity ( $Q_e$ ). No significant changes were noticed between the pH values from 10 to 11. It is evident to see how low adsorptive values of (MB) are occurring in lower levels of pH (pH=2), well as in low alkaline levels of pH (pH=8-9). Therefore, in the low pH range (acidic environment) so the adsorption value is lower, which could be explainable with the numbers of positively charges sites increasing in medium and the numbers of negatively adsorbent material (TW) charged sites decreasing. However, due to the protonation of (MB) in this acid media, (TW) surfaces will become covered with ions (H<sup>+</sup>) is becoming positively charged, this reduces interactions of (MB) ions with (TW) adsorbent negative surfaces and produces electrostatic repulsions between surfaces of the (TW) adsorbent and (MB) cations, preventing formation of bonding between (MB) and (TW) activated area, also which reduce the accessibility of these sites. However, we observe an decreases in the adsorption at the pH values from 6 to 9 (neutral and low basic environment), which cannot be explained without characterizing the (TW) adsorbent material and determining its pH point of zero charge (pHZPC), which indicates that under this pH, (TW) surface charge becomes positively charged but over it, surface charge becomes negatively charged. Moreover, as pH values increases (at high basic environment), the (H<sup>+</sup>) ions concentration decreases and so the adsorption increases. These results can be due to the (TW) material surface which is negatively charged (presence of OH<sup>-</sup> ions) which favors a strong electrostatic force and leads to high interacting of (MB) cations with (TW) adsorbent surfaces. The removing of (MB) could be limited with opposing ions due to the neutralization of (MB) with (H<sup>+</sup>)

ions in high acidic, neutral and low alkaline environments. Maximum (MB) adsorption at higher pH (basic medium) involves equal quantities of both anions and cations being present within this solution, that have been simultaneous neutralised to be adsorbed onto the adsorptive sites of (TW). The (MB) removal efficiency was 81.38% at the pH value of 6 and the highest was 85.10% at the pH value of 11. In addition, for (MB) aqueous solution, the non-controlled pH value without added (TW) was at pH 5.9, almost the same that the pH value of 6 with removal percentage ( $R$ ) of 81.38%. However, the highest removal at the pH value of 11 is just 3.72% greater as compared to elimination at a non-controlled pH at 5.9. Consequently, to reduce the necessity of using (NaOH) again for increasing pH values that could lead to minor changes in disposal efficiencies, the non-controlled pH (5.9) has been retained as the optimum and appropriate value, with a removal percentage ( $R$ ) of 81.38% and an adsorption capacity ( $Q_e$ ) at 4.069 mg.g<sup>-1</sup>. It also explains a better adsorption in basic medium, and these outcomes appear to be close to the ones reported from several author's works in the adsorptive process of (MB) or other cationic dyes on other types of adsorbents.

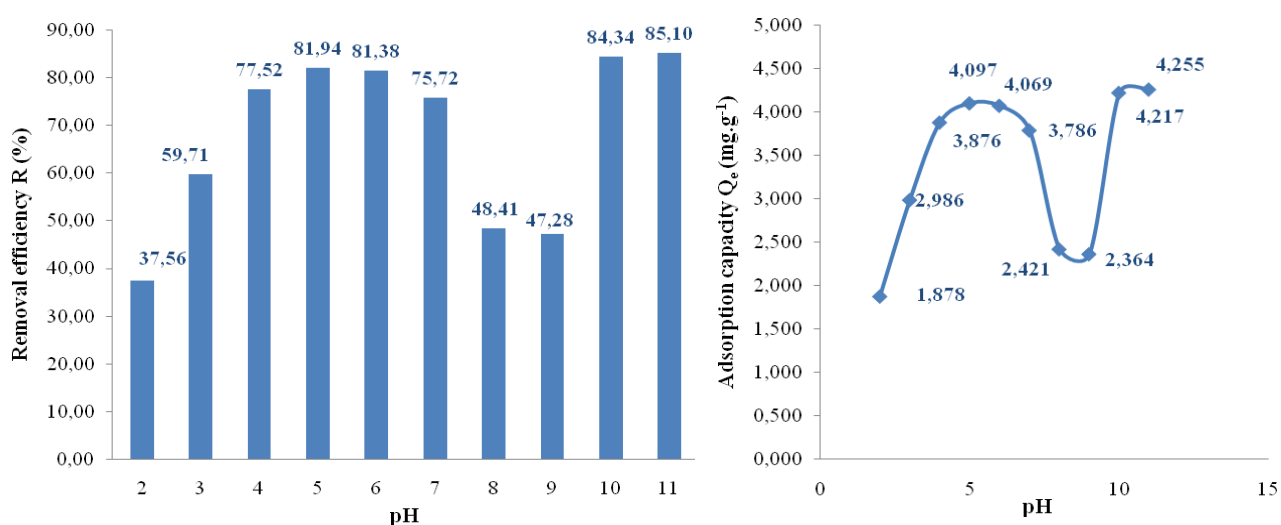


**Figure 4.** (MB) adsorption on (TW) at variable pH's.

### 3.5 (MB) adsorbate initial concentration effect

**Figure 5** shows the variation for (MB) removing along the varied (MB) initial concentration. In terms of ( $R$ ) removal percentage, results demonstrate that the (MB) adsorbed quantity is almost the same, there is no significant difference, whatever the initial concentration of the (MB) solution. Observed removal percentage ( $R$ ) values, are respectively 77.86, 64.70, 75.42 and 78.92 % at 5, 10, 15 and 20 mg.L<sup>-1</sup> initial concentrations. But in terms of adsorption capacity ( $Q_e$ ), (MB) adsorbed quantity increasing gradually when the initial concentration of (MB) solution increases. Observed adsorption capacity ( $Q_e$ ) values, are respectively 1.947, 3.235, 5.657 and 7.892 mg.g<sup>-1</sup> for 5, 10, 15 and 20 mg.L<sup>-1</sup> as (MB) solution initial concentration. This concentration is relating closely with available active sites at the TW adsorbent's surfaces, that is to say, the increasing of the concentration is accelerating adsorbate (MB) diffusion towards the activated area due to the effect of the concentration gradient force. So, we concluded that the adsorptive behaviour is depending of the free sites content of (TW) surface. As a result, a (TW) adsorbent quantity of the value of 1 g can ensure an optimum removal level even for (MB) solutions quantities up to the value of 7.892 mg, with a removal percentage ( $R$ ) the value of 78,92% (corresponding to 20 mg.L<sup>-1</sup> (MB) initial concentration).

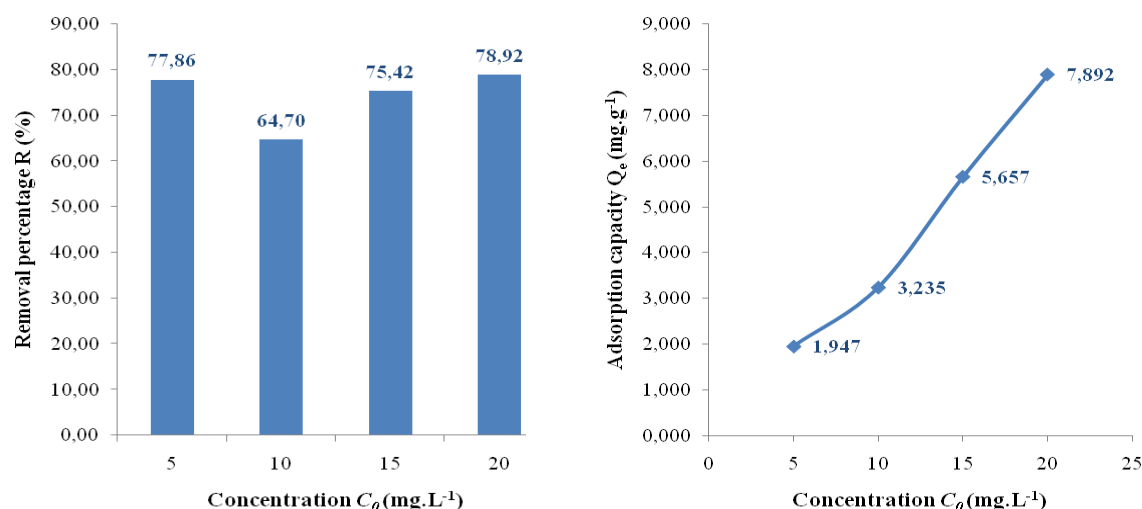


**Figure 5.** (MB) adsorption on (TW) at variable initial concentration.

### 3.6 Modeling adsorption equilibrium

The experimental isotherm of (MB) adsorption by (TW) is given by the curve of ( $Q_e$ ) equilibrium adsorption capacities versus (MB) equilibrium concentrations ( $C_e$ ) (Figure 6). In accordance with the adsorptive isotherm classification adopted by Giles et al., (MB) adsorption on (TW) is of (*S-class*) isotherm, and has a concave form for lower concentrations. This isotherm occurs for (02) reasons, firstly, the forces of solute-solute attraction onto their surfaces can lead to cooperate adsorption leading to the (S)-form, secondly, the adsorption can be prevented by a competitive interaction, especially a complexing reaction to a ligand, in the solution.

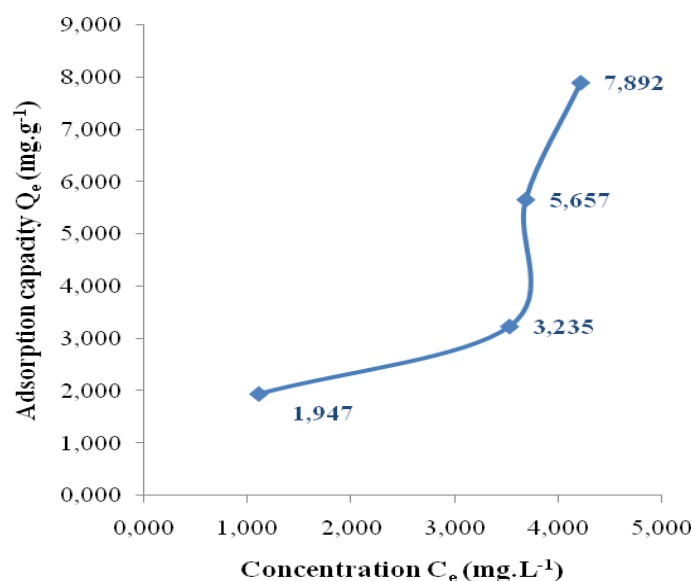


**Figure 6.** Experimental isotherm of the adsorption of (MB) on the (TW).

### 3.7 Modeling adsorption kinetics at equilibrium

The linear curves plotted based on the experimental data of the 3 models are presented in Figure 7 and Table 7 lists data for  $C_0$ ,  $Q_e$ ,  $k_0$ ,  $k_1$ ,  $k_2$ , and  $R^2$ . Calculated correlation coefficients ( $R^2$ ) measured in this study Kinetics models tracings of the Zero-Order, Pseudo-First-Order & Pseudo-Second-Order are respectively of 0,985, 0,975 and 0,998. According to the coefficient of correlation, a high degree of correlation coefficient ( $R^2$ ) was obtained (0,998) for Pseudo-Second-Order one.

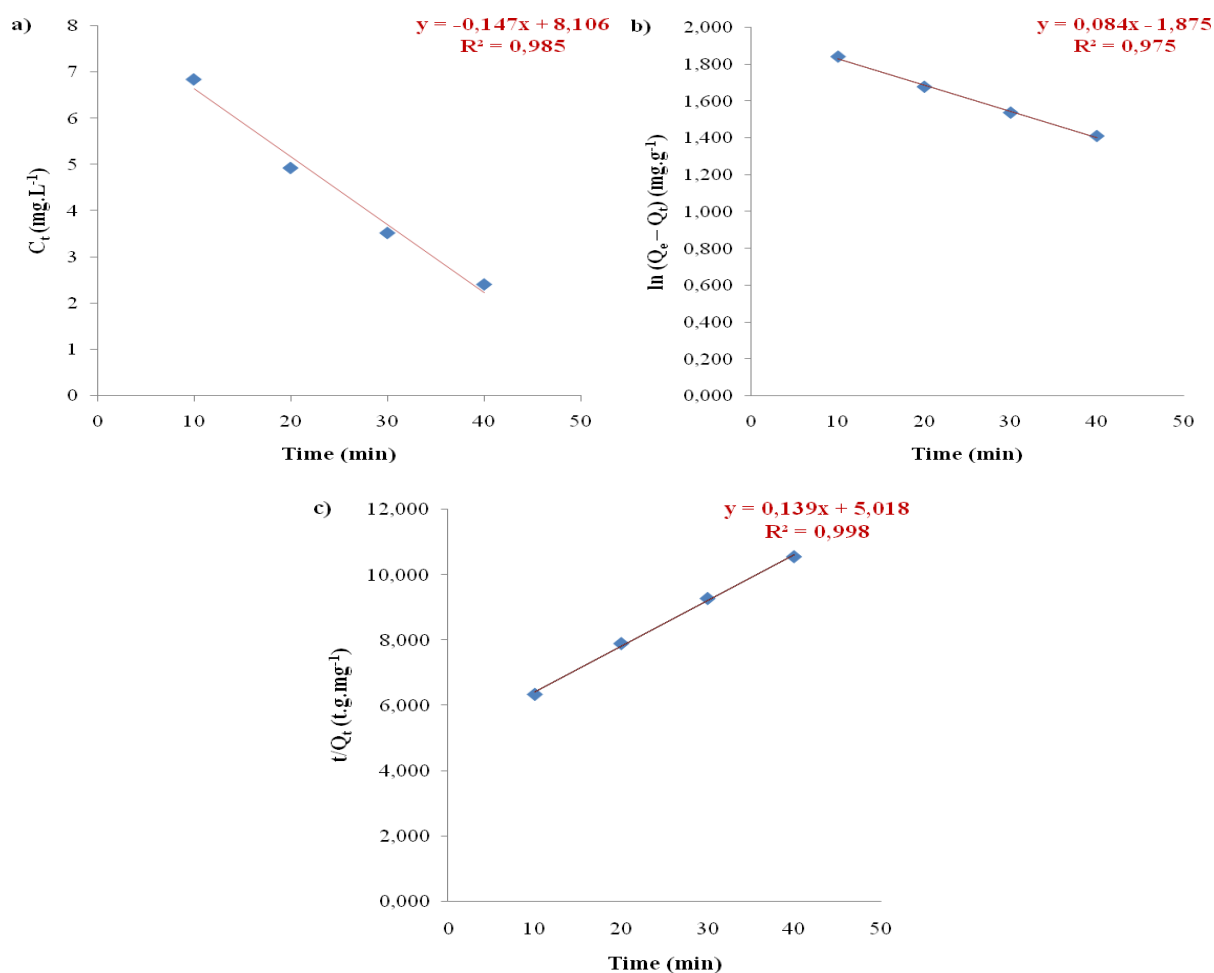


**Figure 7.** (MB) adsorption on (TW) kinetics linear tracings for (a) Zero-Order, (b) Pseudo-First-Order and (c) Pseudo-Second-Order.

**Table 7.** (MB) adsorption on (TW) kinetics models coefficients.

Model	Parameters	
Zero-Order	$R^2$	0.985
	$k_0$ ( $\text{min}^{-1}$ )	0.147
	$C_{0,cal}$ ( $\text{mg.L}^{-1}$ )	8.106
Pseudo-First-Order	$C_{0,exp}$ ( $\text{mg.L}^{-1}$ )	10
	$R^2$	0.975
	$k_1$ ( $\text{min}^{-1}$ )	0.193
Pseudo-Second-Order	$Q_{e,cal}$ ( $\text{mg.g}^{-1}$ )	0.153
	$Q_{e,exp}$ ( $\text{mg.g}^{-1}$ )	7.892
	$R^2$	0.998
	$k_2$ ( $\text{g.mg}^{-1}.\text{min}^{-1}$ )	0.004
	$Q_{e,cal}$ ( $\text{mg.g}^{-1}$ )	7.194
	$Q_{e,exp}$ ( $\text{mg.g}^{-1}$ )	7.892

Also, we can note the fact that using as Kinetic model a Pseudo-Second-Order one ( $Q_{e,cal}$ ) calculated adsorptive capacity at a value of  $7.194 \text{ mg.g}^{-1}$  is considerably closer to ( $Q_{e,exp}$ ) experimental adsorptive capacity at  $7.892 \text{ mg.g}^{-1}$  compared to the Pseudo-First-Order one at  $0.153 \text{ mg.g}^{-1}$ . Furthermore, based on the kinetic profiles, it could be found out a proper fit of the adsorptive mechanism of (MB) on (TW) using as Kinetic model a Pseudo-Second-Order one, obtaining ( $k_2$ ) at  $0.004 \text{ g.mg}^{-1}.\text{min}^{-1}$  and a good ( $R^2$ ) at 0.998.

### 3.8 Modeling adsorption isotherms at equilibrium

Figure 8 show the adsorptive equilibrium values fitting the isotherm models (a) Langmuir and (b) Freundlich. By using Langmuir for (TW), we find linear change at 0.841 as ( $R^2$ ) correlation coefficient. Using Freundlich under similar experimental conditions leads to a linear correlation coefficient ( $R^2$ ) equal to 0.744. By comparing these ( $R^2$ ) coefficients, we observe that for (MB) adsorptive on (TW), for Langmuir ( $R^2$ ) is 0.841 is higher than in Freundlich isotherm model. Table 8 summarizes the characteristics of the adsorptive isotherms and related ( $R^2$ ) values.

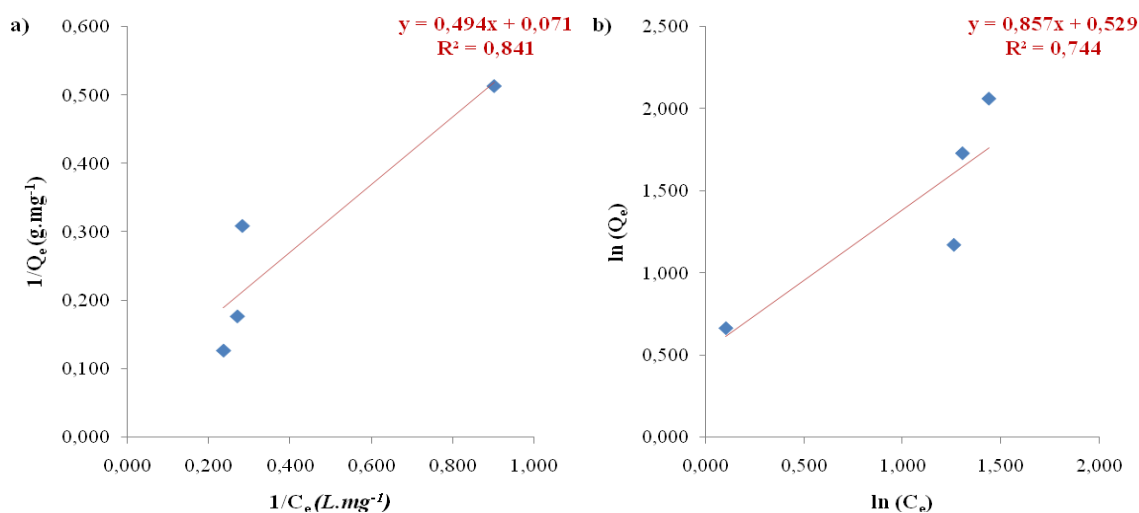


Figure 8. Comparison adsorption isothermal models plots to (MB) adsorptive on (TW), (a) Langmuir, (b) Freundlich.

Table 8. Isothermal characteristics of adsorptive (MB) on the (TW) adsorbent material.

Freundlich				Langmuir			
$1/n$	$n$	$K_F (mg.g^{-1})$	$R^2$	$Q_{m,cal} (mg.g^{-1})$	$K_L (L.mg^{-1})$	$R^2$	$R_L$
0.857	1.167	1.697	0.744	14.085	0.144	0.841	0.258 - 0.582

Higher maximum adsorption capacity calculated ( $Q_{m,cal}$ ) with a value of 14.085  $mg.g^{-1}$  ( $\gg 1$ ) indicating to have very strong adsorbate/adsorbent interaction, it is found to be near the experimental value (7.892  $mg.g^{-1}$ ). This is clear here a more adequate representation of data at equilibrium level via Langmuir compared to Freundlich. Also, high ( $K_L$ ) value (0.144  $L.mg^{-1}$ ) shows that adsorptive levels are much greater compared to desorption in Langmuir. Respectively, it is estimated as Freundlich constants ( $K_F$ ), ( $n$ ) and ( $1/n$ ), are 1.697  $mg.g^{-1}$ , 1.167 and 0.857. Similar to Langmuir, Freundlich isotherm model again indicates favourably adsorptive (MB) on (TW), this was proved by the obtention of a ( $1/n$ ) value lower to 1, indicating that (MB) was easy to be adsorbed. Also, a low value of ( $R^2$ ) in the Freundlich isotherm model was achieved due to its nonlinear adsorptive property ( $1/n$  of 0.857 < 1), particularly under elevated concentration, resulting from saturating (TW) adsorbent free areas on its surface.

Better matching of experimental data to Langmuir's predicts the appearance of a monolayered adsorptive on particular homogeneous adsorptive areas of (MB) to (TW) particles. In order to confirm that the adsorptive is favourable for (MB) on (TW) using the Langmuir isotherm model, the separation factor ( $R_L$ ) is plot versus the (MB) initial concentration ( $C_0$ ), as illustrated in Figure 9. The greatest value 0.582 of ( $R_L$ ) has been reached for 5  $mg.L^{-1}$  that reduces in value to 0.258 for 20  $mg.L^{-1}$ . Either way, ( $R_L$ ) values ranged from 0 to 1 (<1), which approves and suggesting as isotherm model Langmuir one being favourable to (MB) adsorptive onto a (TW).

For the adsorption isotherm analysis, it could be affirmed that adsorptive processing of (MB) on (TW) is best fitted using the Langmuir isotherm model, obtaining an interesting coefficient of correlation ( $R^2$ ) at 0.841. Thus, maximum adsorption capacity calculated ( $Q_{m,cal}$ ) from this model is higher with a value of  $14.085 \text{ mg.g}^{-1}$  ( $\gg 1$ ) indicates a strong adsorbate/adsorbent interaction. However, the values of ( $R_L$ ) were always found in between 0 and 1 ( $< 1$ ), which approves and suggesting Langmuir Langmuir one being favourable to (MB) adsorptive onto a (TW) as isotherm model.

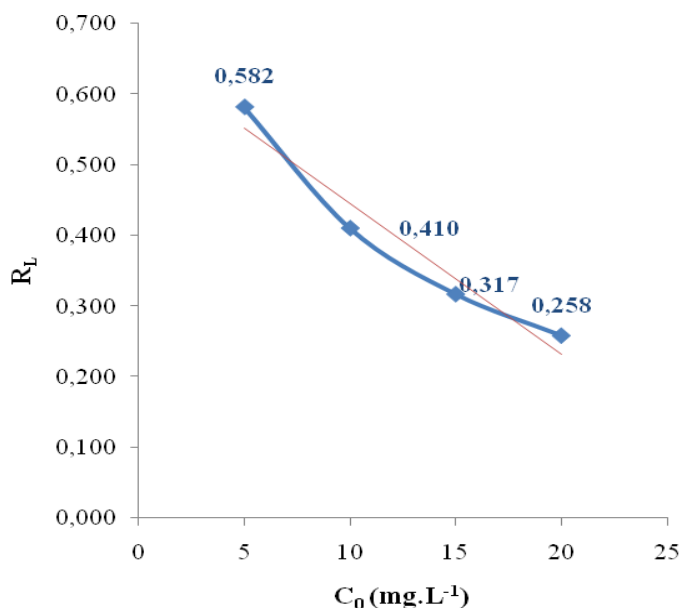


**Figure 9.** Graphic illustration for ( $R_L$ ) separation factor versus ( $C_0$ ) initial concentration of (MB).

## Conclusion

Our studies demonstrate the ability of Tea Wastes (TW) to be a promising and efficient bioadsorbent to remove Methylene Blue (MB) residue from solution. The use of (TW) material like bioadsorbent to remove (MB) gives (02) advantages manner, environmentally in resolving solid wastes disposing problems and from an economic point of view by decreasing the price of treating colored industrial wastewater.

In this context, to obtain the optimum results for (MB) adsorbate removal processing to enhance efficiency, for different variables a batch adsorption experiments are conducted. Optimal conditions for these independent variables achieved if:

- Particles size were around  $125\mu\text{m}$ , with a removal percentage ( $R$ ) at 39.45% and an adsorption capacity ( $Q_e$ ) at  $9.863 \text{ mg.g}^{-1}$ ;
- Contact time was about 40min, with a removal percentage ( $R$ ) of 44.33% and an adsorption capacity ( $Q_e$ ) at  $11.083 \text{ mg.g}^{-1}$ ;
- Adsorbent dose was 0.04g, having a removal percentage ( $R$ ) to 66.35% and an adsorption capacity ( $Q_e$ ) at  $4.147 \text{ mg.g}^{-1}$ ;
- Uncontrolled pH in 5.9 was maintained as the optimum, with a removal percentage ( $R$ ) of 81.38% and an adsorption capacity ( $Q_e$ ) to  $4.069 \text{ mg.g}^{-1}$ ;
- An adsorbent quantity with the value of 1g can ensure an optimum removal level for adsorbate quantities up to the value of 7.892mg (corresponding to MB initial concentration at  $20 \text{ mg.L}^{-1}$ ), in addition to ( $R$ ) removal percentage at 78.92% and ( $Q_{m,exp}$ ) as maximum experimental adsorption capacity at  $7.892 \text{ mg.g}^{-1}$ .



Results demonstrate an adsorption behavior in accordance with an isotherm (*S-class*), for an experimental adsorption capacity ( $Q_{e,exp}$ ) of 7.892 mg.g<sup>-1</sup>. Furthermore, a best fitting of kinetic values by Pseudo-Second-Order may conclude regarding its adsorptive mechanism, obtaining an excellent correlation coefficient ( $R^2$ ) at 0.998, and an estimated adsorption capacity ( $Q_{e,cal}$ ) to 7.194 mg.g<sup>-1</sup>, closely related to experimentation. For the adsorptive isotherm analysis, it could be affirmed for adsorptive action a best fitted using the Langmuir isotherm model, obtaining a good correlation coefficient ( $R^2$ ) with a value of 0.841. However, the values of ( $R_L$ ) found in between 0 and 1, which approves and suggesting the Langmuir isotherm model to be favourable for this adsorption case.

It is concluded a successful application of (TW) to remove (MB) through adsorption. Considering these positive promising achieved outcomes, this preliminary work promotes and indicates the potential use of these inexpensive adsorbent products in order to treating real wastewater with great adsorptive performance.

Finally, postulating adsorptive mechanism from the perspective of desorption is rarely discussed. Comprehensive reusability studies involving (TW) desorption, regeneration and adsorption cycles are also still lacking in the literature. For this purpose, with a view to the horizon, before further application in real textile dye and real effluent treatment, our future works will include studies to explore the profile of (TW) Adsorbent regeneration and (TW) Adsorbent recycle.

## References

- Ahmed M. B., Zhou J. L., Ngo H. H., Guo W., Thomaidis N. S., Xu J. (2017) Progress in the biological and chemical treatment technologies for emerging contaminant removal from wastewater: A critical review, *J. Hazard. Mater.*, 323(A), 274-298. <https://doi.org/10.1016/j.jhazmat.2016.04.045>.
- Ait Hmeid H., Akodad M., Baghour M., Moumen A., Skalli A., Azizi G., Anjjar A., Aalaoul M., Daoudi L. (2021) Adsorption of a basic dye, Methylene Blue, in aqueous solution on bentonite, *Mor. J. Chem.*, 9(3), 416-433. <https://doi.org/10.48317/IMIST.PRSM/morjchem-v9i3.23303>.
- Akartasse N., Azzaoui K., Mejdoubi E., Hammouti B., Elansari L.L., Abou-salama M., Aaddouz M., Sabbahi R., Rhazi L. and Sijaj M. (2022) Environmental-Friendly Adsorbent Composite Based on Hydroxyapatite/Hydroxypropyl Methyl-Cellulose for Removal of Cationic Dyes from an Aqueous Solution, *Polymers*, 14(11), 2147; <https://doi.org/10.3390/polym14112147>
- Alam M. Z., Anwar A. F., Heitz A. (2018) Removal of Nutrients from Stormwater Using a Mixed Biochar-Alum Sludge Adsorbent, *10<sup>th</sup> International Conference on Water Sensitive Urban Design, Engineers Australia*. <http://hdl.handle.net/20.500.11937/68152>.
- Alam Z., Bari N., Kawsari S. (2022) Statistical optimization of Methylene Blue dye removal from a synthetic textile wastewater using indigenous adsorbents, *Environ. Sustain. Indic.*, 14, 100176-100189. <http://dx.doi.org/10.1016/j.indic.2022.100176>.
- Arumai P. J. D., (2008) Study on Removal of COD and Colour from Textile Wastewater Using Limestone and Activated Carbon, *M. Sc. Thesis., University Sains Malaysia*.
- Boumya W., Khnifira M., Abdennouri M., Achak M., Barka N. (2021) Theoretical investigation of the mechanism, chemo-and stereospecificity in Box-Behnken design for the optimization of methylene blue and methyl orange removal from aqueous solution by activated carbon, *Mor. J. Chem.*, 9(1), 123-131. <https://doi.org/10.48317/IMIST.PRSM/morjchem-v9i1.19953>.
- Collivignarelli M.C., Abbà A., Miino M.C., Damiani S. (2019) Treatments for color removal from wastewater: State of the art, *J. Environ. Manag.*, 236, 727-745. <https://doi.org/10.1016/j.jenvman.2018.11.094>.
- Crini G., (2006) Non-conventional low-cost adsorbents for dye removal: a review, *Biores. Technol.*, 97(9), 1061-1085. <https://doi.org/10.1016/j.biortech.2005.05.001>.
- Crini G., Lichtfouse E. (2019) Advantages and disadvantages of techniques used for wastewater treatment. *Environ. Chem. Lett.*, 17, 145-155. <https://doi.org/10.1007/s10311-018-0785-9>.

- El-Bindary A. A., Hassan N., Shahat A., El-Didamony A., El-Desouky M. G., (2020) Equilibrium, Kinetic and Thermodynamic studies of adsorption of cationic dyes from aqueous solution using ZIF-8, *Mor. J. Chem.*, 8(3), 627-637. <https://doi.org/10.48317/IMIST.PRSM/morjchem-v8i3.21127>.
- Elmontassir H., El Falaki K., Afdali M., Karhat Y. (2019) Adsorption of a dye and a real rejection of textile on sludge from drinking water treatment, *Mor. J. Chem.*, 7(3), 493-505. <https://doi.org/10.48317/IMIST.PRSM/morjchem-v7i3.15882>.
- Elsherif K. M., El-Dali A., Ewlad-Ahmed A. M., Treban A. A., Alqadhi H., Alkarewi S., (2022) Kinetics and Isotherms Studies of Safranin Adsorption onto Two Surfaces Prepared from Orange Peels, *Mor. J. Chem.*, 10(4), 639-651. <https://doi.org/10.48317/IMIST.PRSM/morjchem-v11i1.32137>.
- Franca A.S., Oliveira L.S., Ferreira M.E. (2009) Kinetics and equilibrium studies of methylene blue adsorption by spent coffee grounds, *Desalination*, 249(1), 267-272. <https://doi.org/10.1016/j.desal.2008.11.017>.
- Freundlich H., (1906) Über die adsorption in losungen, *Z. Phys. Chem.*, 57U(1), 385-470.
- Giles C. H., Smith D., Huitson A. (1974) A general treatment and classification of the solute adsorption isotherm. I. Theoretical, *J. Colloid Interface Sci.*, 47(3), 755-765.
- Gupta V. K., Suhas (2009) Application of low-cost adsorbents for dye removal-A review, *J. Environ. Manag.*, 90(8), 2313-2342. <https://doi.org/10.1016/j.jenvman.2008.11.017>.
- Hamad H. N., Idrus S. (2022) Recent Developments in the Application of Bio-Waste-Derived Adsorbents for the Removal of Methylene Blue from Wastewater: A Review, *Polymers*, 14(4), 1-39. <https://doi.org/10.3390/polym14040783>.
- Han R. P., Wang Y. F., Han P., Shi J., Yang J., Lu Y. S. (2006) Removal of methylene blue from aqueous solution by chaff in batch mode, *J. Hazard. Mater.*, 137(1), 550-557. <https://doi.org/10.1016/j.jhazmat.2006.02.029>.
- Hassan M. M., Carr C. M. (2021) Biomass-derived porous carbonaceous materials and their composites as adsorbents for cationic and anionic dyes: A review, *Chemosphere*, 265, 129087. <https://doi.org/10.1016/j.chemosphere.2020.129087>.
- Hassanein T. F., Koumanova B. (2010) Evaluation of adsorption potential of the agricultural waste, wheat straw for basic yellow 21, *J. Univ. Chem. Technol. Metall.*, 45(4), 407-414.
- Holkar C., Jadhav A., Pinjari D. V., Mahamuni N. M., Pandit A. B. (2016) A critical review on textile wastewater treatments: Possible approaches, *J. Environ. Manag.*, 182, 351-366. <https://doi.org/10.1016/j.jenvman.2016.07.090>.
- Hummadi K. K., Luo S., He S. (2022) Adsorption of methylene blue dye from the aqueous solution via bio-adsorption in the inverse fluidized-bed adsorption column using the torrefied rice husk, *Chemosphere*, 287(1), 1-11. <https://doi.org/10.1016/j.chemosphere.2021.131907>.
- Kali A., Dehmani Y., Loulidi I., Amar A., Jabri M., El-kord A., Boukhlifi F. (2022) Study of the adsorption properties of an almond shell in the elimination of methylene blue in an aquatic, *Mor. J. Chem.*, 10(3), 509-522. <http://dx.doi.org/10.48317/IMIST.PRSM/morjchem-v10i3.33140>.
- Koyuncu I., Güney K. (2013) Membrane-Based Treatment of Textile Industry Wastewaters, *Encycl. Membr. Sci. Technol.*, 1-12. <https://doi.org/10.1002/9781118522318.EMST127>.
- Langmuir I. (1916) The constitution and fundamental properties of solids and liquids. Part I. Solids, *J. Am. Chem. Soc.*, 38(11), 2221-2295.
- Loulidi I., Boukhlifi F., Ouchabi M., Amar A., Jabri M., Kali A., Chraïbi S., Hadey C., Aziz F. (2020) Adsorption of crystal violet onto an agricultural waste residue: kinetics, isotherm, thermodynamics, and mechanism of adsorption, *Sci. World J.*, 1-9. <https://doi.org/10.1155/2020/5873521>.
- Mejbar F., Miyah Y., El Badraoui A., Nahali L., Ouissal A., Khalil A., Zerrouq F. (2019) Studies of the adsorption kinetics process for removal of methylene blue dye by residue of grenadine bark extraction, *Mor. J. Chem.*, 6(3), 436-443.
- Muhammad A. S., Abdurrahman M. A. (2020) Adsorption of methylene blue onto Modified Agricultural Waste, *Mor. J. Chem.*, 8(2), 412-427. <https://doi.org/10.48317/IMIST.PRSM/morjchem-v8i2.16692>.
- Mulushewa Z., Dinbore W. T., Ayele Y. (2021) Removal of methylene blue from textile waste water using

